Mechanical characterization of 3D printed samples under vibration: Effect of printing orientation and comparison with subtractive manufacturing

Philippe Lesage, Lucas Dembinski, Remy Lachat, Sébastien Roth

Version of Record: https://www.sciencedirect.com/science/article/pii/S2590123022000421
Manuscript_e5fadcf9af3d79e0513e4bf196f415e9

Mechanical characterization of 3D printed samples under vibration: effect of printing orientation and comparison with subtractive manufacturing

Philippe LESAGE*, Lucas DEMBINSKI, Remy LACHAT, Sébastien ROTH

Laboratoire Interdisciplinaire Carnot de Bourgogne, site UTBM, UMR 6303, CNRS / Univ. Bourgogne Franche-Comté

*Corresponding authors: sebastien.roth@utbm.fr

KEYWORDS

Dynamic characterization, vibration, printing effect, orientation effect, additive manufacturing

ABSTRACT

This paper describes dynamical characterization of mechanical structures manufactured by Selective Laser Melting (SLM) process at various orientations. The samples are also compared to subtractive component. The additive metal samples were manufactured by a 3D printer (Renishaw AM 250, Renishaw) and were tested using vibration analysis of embedded-free beam installation. Experimental setup was replicated using the same geometry of samples printed at various orientations and submitted to low velocity impact. Accelerometers allowed recording mechanical responses of all the specimens, allowing characterizing the dynamic behavior of each component and the effect of the printing orientation and printing angles.

INTRODUCTION

Additive manufacturing (AM) is more and more used in the context of mechanical component development allowing developing various structures which could not be designed with other classical process. Indeed, lots of scientific studies of the literature have highlighted trends and opportunities concerning this process, and some benefits that it could bring for several fields of industries [1, 2, 3, 4, 5].
Whereas the physical process is widely studied in the literature, the results of the mechanical components in terms of specifications is less understood, and lots of work need to be conducted to investigate the real behavior and the efficiency of such structures. Indeed, like for classical process, the components manufactured by additive process need to be mechanically characterized to analyze if they satisfy the requirements, especially for strength, and mechanical constraints. Thus, recent studies of the literature interest in the characterization of such materials:
the behavior of additive manufactured (AM) structures like in the work of Maconachie et al. (2020) [6] regarding the effect of build orientation and the static and dynamic response of SLM AlSi10Mg.

Feng et al. (2018) [7], investigated Ti6Al4V lattice structures manufactured with SLM selective laser melting

In the specific framework of dynamic characterization, interesting works can be found in the literature, such as the work of Asgari et al. (2018) [8] who studied the dynamic mechanical behavior of the AlSi10Mg_200C samples using a Split Hopkinson Pressure Bar (SHPB). Andrew et al (2021), investigated plate lattice stereolithography AM specimens and performed drop weight impact to evaluate energy absorption characteristics.[9]. Dynamic stiffness was of interest in the work of Betters et al. (2020) who measured frequencies and damping characteristics in material manufactured with metal wire arc additive

process [10]. Dynamic shear-compression response of Ti6Al4V specimens was investigated by Fadida et al. (2020) [11]. Atypical nacre-like composites material was characterized under drop weight impact loading by Ko et al. (2020) [12]. Ling et al. (2019) explored dynamic compressive behavior of lattice structures manufactured with polymer resins [13]. Charpy impacts were conducted by Komarasamy et al. (2019) on additively manufactured nickel alloy 718 [14]. Hadadzadeh et al. (2019) explored the effect of microstructure of additively manufactured AlSi10Mg on dynamic loading behavior [15]. In addition to microstructure, the porosity was also a point of interest in the study of Babamiri et al. (2020), who studies the effect of these parameters on the dynamic behavior of additively manufactured Inconel 718 [16]. Dynamic compression tests were performed by Chen et al. (2021) on 316L stainless steel manufactured by an additive manufacturing process to explore Dynamic mechanical properties [17]. At a macroscopic level, Lesage et al. (2018) compared the global behavior of aluminum AlSi10Mg manufactured with SLM process and subtractive electrical discharge process [18] under vibrations.

Classical methods are used in the literature to characterized such materials. Atypical ones can also be found such as studies of Hastie et al. 2020, Hastie et al. 2021 and Koeblin et al. 2022, who explored the mechanical characteristics and pores in the materials at microscopic level, including 3D X-ray micro computed tomography [19-21].

Low strain rate impact behavior of ABS material was studied by Hadidi et al. (2019) using drop test and Charpy impact pointing out the effect of peening frequency and printing orientation on the ability to absorb energy [22]. The latter parameter is also of great interest in the characterization of mechanical structures, since there are infinite possibilities of printing orientations of the mechanical components. Studies of the literature have begun to investigate this point.

Hitzler et al. 2017 [23] conducted investigations on the effect of the direction and location of selective laser melted AlSi10Mg specimens and revealed significant variation of mechanical properties.

For biomedical application, Maroti et al. 2018, concluded in his study that the orientation of 3D printing affects the mechanical properties of the printed objects leading to anisotropy [24]. Honarmandi et al. 2019, concluded to a significant effect of the printing orientation which need to be taken into account for mechanical properties optimization for ABS material [25]. According to the literature, and concerning additive process, the concept of anisotropy and heterogeneity are of great interest and have an essential role in the understanding of mechanical behavior of 3D components, at macroscopic and microscopic scale [26]. In that context, the printing parameters are essential, and specifically the printing orientation.

Finally, the understanding of dynamic behavior of additive samples are of huge importance in order to deploy the technology in various field of mechanical industry, such as automotive or defense industries, where the dynamic behavior play an essential role.

In the framework of mechanical characterization of 3D components under dynamic loadings, we propose in this study to investigate the effect of the printing orientation on the dynamic response of metallic specimen manufactured via Selective Laser Melting process. Thus, all the specimen, as well as a subtractive samples taken as a reference, are submitted to low-amplitude vibrations using an impact hammer. Accelerations, eigen frequencies, damping effects, energetic absorption of each specimen are recorded in order to investigate their dynamic behavior and their differences.

Finally, this study contributes to the understanding of mechanical behavior of structures manufactured by SLM under dynamical loadings, and provide some interesting results related to the effect of the printing orientation.

MATERIAL AND METHOD

This study focuses on the dynamic behavior of additive manufactured specimen, and also a subtractive sample, which is considered as the reference. The framework of this study is a continuity of already published work (Lesage et al. [18]), where low velocity impacts were used to load a mechanical component, to identify existing difference between 3D components, and classical subtractive component.

Similar methods are used in the present study, and can be described as follow:
The first step consists in the printing of the specimen on a SLM 3D printer Renishaw AM 250 ©. Various orientations of the specimen were chosen in order to identify their effects on the mechanical behavior. Secondly, these specimen were tested under low velocity vibrations using an impact hammer. All the specimens were clumped on one extremity. Accelerometers were placed in the other extremity of the samples. Input force sensors were placed in the middle of the experimental device at the impact location, in order to evaluate the input impact force.
An illustration of the flowchart of the analysis is provided in figure 1.

The experiment is based on the comparison of the frequency responses to dynamic stresses carried out with an impulse hammer, to evaluate and highlight the different characteristics between subtractive and additive processes.
The samples from the subtractive process were taken from an AlSi10Mg foundry ingot. The same ingot was also used to manufacture the powder, which was used to build the additive specimens. The 3D samples were printed in one single printing process, on a single plate, so that all the specimens were manufactured using the same material powder. Finally, the composition of the samples resulting from additive and subtractive processes was thus guaranteed to be the same.
Three different sets of additive samples were printed: Flat Printing Orientation, Upright Printing Orientation and Rotation Printing Orientation, as illustrated in figure 2. For these three different printing directions, 7 different samples were printed, with different incident angle: 0° to 90 ° with 15° increment. Then, comparisons were possible to investigate the effect of the printing direction, as well as the effect of angle in a specific printing way (figure 2 and table 1)

Accelerometers have been placed in the input area in order to record the input loading, as well as to ensure that no lateral loadings exist, as illustrated in figure 3.
A serie of 258 impacts have been conducted. With an aim of obtaining the same input for all the impacts, allowing comparisons with equivalent inputs, 200 impacts were analyzed, and presented an input force of 250 N +/-1%. For each series, almost 10 temporal responses were recorded, allowing obtaining 10 responses per specimen, providing a significant average. Recordings were made with a built-in anti-aliasing filter, at 10 kHz sampling rate. The software used for the post processing data was EDASWIN.

RESULTS

Frequency analysis: Intra comparison between Upright, Flat, Rotation configurations.

The following figure 4, illustrates results of additive components coming from the Flat print configuration, Upright print configuration, and Rotational print configuration for 0°, 45°, 90°.
Figure 4a illustrate differences between angle (0°, 45°, 90°) for flat printing orientation.
Figure 4b illustrate differences between angle (0°, 45°, 90°) for rotation printing orientation.
Figure 4c illustrate differences between angle (0°, 45°, 90°) for rotation printing orientation
In addition, results from subtractive specimens, are also provided for all the experiments.
It should be mentioned that only the results of 3 angles have been pointed out here, for more visibility. The three first eigen frequencies are illustrated, coming from classical FFT analysis.

Frequency analysis: Inter comparison for the three various orientation printing at three given angles: 0°, 45°, 90°

The three first eigen frequencies are illustrated, for additive components and subtractive one.
Figure 5a illustrate differences between flat, rotation, and upright printing orientation for a given angle (0°).
Figure 5b illustrate differences between flat, rotation, and upright printing orientation for a given angle (45°).
Figure 5a illustrate differences between flat, rotation, and upright printing orientation for a given angle (90°).

By convention, the first eigen frequency is the nodeless mode M_0, the second eigen frequency is the one node mode M_1 and the third eigen frequency is the two-nodes mode M_2.

The following table 2 gather all the natural frequencies for various angle and various printing orientations.

The first mode M0 (Nodeless mode) of all specimens is located in a spectral range between 125 and 150 Hz with excellent experimental repeatability regardless of the printing orientation. The second mode M1 of all specimens (one node mode) is located in a spectral range between 800 and 1100 Hz. It can also be noticed that the 2nd eigen frequencies for Flat, Upright, Rotate and subtractive specimens M1 frequencies peaks have high amplitude like those of the 1st mode M0. Rotate and Upright responses are at the same frequency at 0° (991 HZ) and 90° (964 Hz) orientation. Flat print response has higher frequency level (920 to 839 Hz) compared to subtractive sample and lower frequency level compared to Rotate and upright print (1000 Hz). The third mode of all specimens is located in a spectral range between 2435 and 2873 Hz. M2 frequencies have lower amplitude than M0 and M1 mode. Figure 6 shows that the trend of frequency evolution as a function of the printing angle is the same whatever the observed mode. Concerning Rotate and Upright orientation, we can notice that eigen frequencies M0, M1 and M2 are superimposed for 0° and 90° angle.

Damping analysis:

The following curves of figure 7, illustrate the damping behavior of the samples.

Figure 7a illustrates a comparison between samples for flat printing orientation at different angles.

Figure 7b is the global comparison for the three printing orientations at different angles.

All the curves also provide subtractive sample for comparisons.

From the temporal recording, the envelope curves of the signals have been extracted, and illustrate a significant difference between subtractive and additive processes (figure 7). It can be observed that the curve dedicated to the damping is lower for subtractive samples compared to additive ones (figure 7a), leading to a higher damping coefficient, as illustrated in figure 7b.

It can also be noticed that the damping ratio for rotate and upright orientation have the same value for 90° angle.

Impact and wave velocity.

Figure 8 illustrates the time delay between the input and the accelerometer output located at the extremity of the samples.

Figure 8a illustrates, for flat printing configuration, the time delay for various angle (0°, 45°, 90°).

Figure 8b illustrates, for Upright printing configuration, the time delay for various angle (0°, 45°, 90°).

The following table 3 shows the time interval between input and outputs for the three printing orientations and for various angles, followed by the global representation of time intervals for the three printing orientations and various angles (figure 9).

Figure 8a shows the time delay between impulse and Flat printing for three configurations angle: 0°, 45°, 90°. It can be noticed that the 0° flat printing has the fastest response, followed by the 45° and the 90° angle.

In figure 8b, the time delay between impulse and Upright printing for three configurations angles (0°, 45°, 90°) is illustrated. The three configuration angles lead to the same results.

Figure 8c illustrate a higher time delay for the Rotation printing orientation configuration with a 45° angle, whereas 0° and 90° are almost superimposed.

Figure 9 which is the inter and intra comparison between the different specimens, illustrates the time delay evolution trends according to the printing orientations as well as the different angles.

DISCUSSION

This study focuses on the comparison of metallic specimens manufactured according two processes:

an additive process (SLM) with the particularity of specimen printed in seven different directions, 0° to 90° in steps of 15° and along three axes as illustrated in figure 2, and a subtractive process (conventional machining) where the specimens are taken from foundry ingots in AlSi10Mg which were also used to manufacture all the additive specimens of this study.

Frequency responses have been provided in the results section for different printing configurations and various printing angles. Significant discrepancies can be observed according to the printing orientation for second M1 mode and third M2 mode, whereas M0 is almost identical for the three printing orientations whatever is the angle.

It is of interest to consider that the differences between modes M1 and M2 are mainly due to the structural heterogeneities which are spread randomly along the length and thickness of the sample; these can be generated by printing defects such as powder gaps, holes or unmelted lines of powder. This cause ranges of heterogeneities which influence the frequency response as well as the deformation modes. According to the theory [27, 28], the higher frequency leads to the higher stiffness. Indeed, Eigen frequencies are the combination of a term $\sqrt{\frac{E}{\rho}}$ characterizing the intrinsic properties of material (elasticity E, inertia ρ) which is identified with the speed of sound propagation in the beam and a geometric term $\frac{1}{L^2}\sqrt{\frac{I}{S}}$ which characterizes the geometry of the structure. (L=length, I= Area moment of inertia, S=section of the beam). Finally, the stiffness of the samples can be evaluated (figure 6) according to the printing orientation: Flat printing with the highest stiffness, followed by Upright and Rot printing.
It is worth to be noticed that the 90° angle for the upright printing orientation has similar behavior than the 90° angle for rotation printing orientation. Both specimens have similar manufacturing conditions and give identical results in terms of frequencies with regards to the orientation and the angles, as illustrated in figure 2. This point is also valid for other parameters such as the damping ratio and the time delay. This comment is relevant concerning the reproducibility of the measurements, and also the process reliability.

A correlation may exist between the time delay and the damping ratio. The pathway of the wave in the specimen will be different and the wave will need more or less time to reach the extremity of the sample (recorded by the accelerometer in the extremity), depending on the printing orientation and also the angle. The variation of the laser path on the SLM, will generate some specific path, which, in addition to heterogeneity and anisotropy of the material, will modify the travel of the wave. Heterogeneities lead to a spatial density gradient, which influences the speed of wave propagation [29, 30, 31, 32].

The investigation of the measurement of the time delay between the impulse and the specimen's response concern both the reaction time of the specimen, and the internal structure (viscous friction which governs the damping). Significant differences can be shown in table 3 and figure 9, concerning the time delay. According to our results, whatever is the printing orientation and the angles, only the case Flat specimen at 0° has a lower value than the value of the subtractive specimen, which is the reference (0.2688 ms versus 0.3005 ms respectively). In the study It should also be noticed that the specimen Flat at 90° has the highest value (0.5881 ms), which could be explained by the type of deposits of the layers in the process, which lead to differences in terms of the wave's path. This comment can make the link with the different printing lines built by the path of the fusion laser which lead the waves toward various spatial directions, which may explain the differences in terms of time delay. The following figure 10 illustrates this comment.
Several perspectives can be drawn, at short terms, to complete the present study:
The different samples have been submitted to low-velocity impacts with the shock hammer, to remain under plasticity domain. This work has to be extended for other loading cases, and especially to reach plastic domain until material rupture.
It is also of interest to point out that results are representative of samples printed according to various orientation and angles for a specific machine. Other SLM machine should be used to compare data to the present results and to generalize the results.
In addition, an investigation at a microscopic level, would contribute to the investigation of the different microstructures for various printing. This step is also under progress. The microstructural analysis (such as the study of Tridello et al. 2020 [33]) can also help to develop micro-macro relationships for the

development of adequate constitutive laws to be implemented in a numerical code.
It also of interest to point out that the present study investigates the frequency analysis of the samples, which can clearly lead to a more complete structural analysis. Indeed, classical Rayleigh theory can then be applied on this precise configuration of the beam, and which could make the link between the frequencies and the Young modulus. Thus, for each frequency obtained for each printing orientations and angles (and illustrated in table 2), a corresponding elasticity coefficient could be provided illustrating the significant variation of the mechanical properties of the samples as already conducted in the literature [34, 35, 36] and highlighting the significant effect of the printing configuration.

Finally, all these steps can help analysing the mechanical behavior of 3D printed samples in order to provide benefits and drawbacks of each printing configuration, and also guidelines for adequate printing which respect mechanical requirements.

CONCLUSION

This study is a new step in the understanding of additive manufactured component submitted to low velocity impact. AM specimen manufactured according to different orientations (Flat, Upright and Rotate) and different angles (0° to 90° in steps of 15°) were compared to a subtractive specimen manufactured from an AlSiMg10 ingot. Significant differences exist between the different samples in terms of frequency study, damping ratio and relative time delay. For the same input and test configurations, AM specimens have significant difference responses due the different printing orientations and angles.

REFERENCES

[1]	Al Rashid A., Khan S. A., Al-Ghamdi S. G., Koç M., Additive manufacturing: Technology, applications, markets, and opportunities for the built environment, Automation in Construction, Volume 118, 2020, 103268,
[2]	M. K. Thompson, G. Moroni, T. Vaneker, G. Fadel, R. I. Campbell, I. Gibson, A. Bernard, J. Schulz, P. Graf, B. Ahuja, F. Martina, Design for Additive Manufacturing: Trends, opportunities, considerations, and constraints, CIRP Annals, Volume 65, Issue 2, 2016, Pages 737-760,
[3]	P.S. Ghahfarokhi, A. Podgornovs, A. Kallast, A. J. Marques Cardoso , A. Belahcen, T. Vaimann, H. Tiismus, B. Asad "Opportunities and Challenges of Utilizing Additive Manufacturing Approaches in Thermal Management of Electrical Machines," in *IEEE Access*, vol. 9, pp. 36368-36381, 2021,
[4]	A.Zocca, , P.Colombo, , C.M.Gomes, and J.Günster, (2015), Additive Manufacturing of Ceramics: Issues, Potentialities, and Opportunities. J. Am. Ceram. Soc., Vol. 98: Issue 7 July 2015 Pages 1983-2001. https://doi.org/10.1111/jace.13700
[5]	S.Babu , L.Love , R.Dehoff, W.Peter, T.Watkins,, S.Pannala, (2015). Additive manufacturing of materials: Opportunities and challenges. MRS Bulletin, 40(12), 1154-1161. doi:10.1557/mrs.2015.234
[6]	T. Maconachie, M. Leary, J. Zhang, A. Medvedev, A. Sarker, D. Ruan, G. Lu, O. Faruque, M. Brandt, Effect of build orientation on the quasi-static and dynamic response of SLM AlSi10Mg, Materials Science and Engineering: A, Volume 788, 2020, 139445,
[7]	Q.Feng, Q.Tang, Y.Liu, R.Setchi, S.P. Soe, S.Ma, L.Bai Quasi-static analysis of mechanical properties of Ti6Al4V lattice structures manufactured using selective laser melting. Int J Adv Manuf Technol 94, 2301–2313 (2018).
[8]	H. Asgari, A. Odeshi, K. Hosseinkhani, M. Mohammadi a On dynamic mechanical behavior of

	additively manufactured, AlSi10Mg_200C, Materials Letters 211 (2018) 187–190
[9]	J J. Andrew, J. Schneider, J. Ubaid, R Velmurugan, N K Gupta, S Kumar, Energy absorption characteristics of additively manufactured plate-lattices under low- velocity impact loading, International Journal of Impact Engineering, Volume 149, 2021, 103768
[10]	E.D. Betters, J. West, M. Noakes, A. Nycz, S. Smith, T. L. Schmitz, Dynamic stiffness modification by internal features in additive manufacturing, Precision Engineering, Volume 66, 2020, Pages 125-134
[11]	R. Fadida, A. Shirizly, D. Rittel, Static and dynamic shear-compression response of additively manufactured Ti6Al4V specimens with embedded voids, Mechanics of Materials, Volume 147, 2020, 103413
[12]	K. Ko, S. Jin, S. E. Lee, J.-W. Hong, Impact resistance of nacre-like composites diversely patterned by 3D printing, Composite Structures, Volume 238, 2020, 111951
[13]	C.Ling, A. Cernicchi, M. D. Gilchrist, P. Cardiff, Mechanical behaviour of additively-manufactured polymeric octet-truss lattice structures under quasi-static and dynamic compressive loading, Materials & Design, Volume 162, 2019, Pages 106-118
[14]	M. Komarasamy, S.Shukla, S.Williams, K. Kandasamy, S. Kelly, R. S. Mishra, Microstructure, fatigue, and impact toughness properties of additively manufactured nickel alloy 718, Additive Manufacturing, Volume 28, 2019, Pages 661-675
[15]	A. Hadadzadeh, B. S. Amirkhiz, A. Odeshi, J. Li, M. Mohammadi, Role of hierarchical microstructure of additively manufactured AlSi10Mg on dynamic loading behavior,
	Additive Manufacturing, Volume 28, 2019, Pages 1-13
[16]	B. B. Babamiri, J. Indeck, G. Demeneghi, J. Cuadra, K. Hazeli, Quantification of porosity and microstructure and their effect on quasi-static and dynamic behavior of additively manufactured Inconel 718, Additive Manufacturing, Volume 34, 2020, 101380
[17]	J. Chen, H. Wei, K. Bao, X. Zhang, Y. Cao, Y. Peng, J. Kong, K. Wang, Dynamic mechanical properties of 316L stainless steel fabricated by an additive manufacturing process, Journal of Materials Research and Technology, Volume 11, 2021, Pages 170-179
[18]	P. Lesage, L. Dembinski, M. Schmitt, J.-P. Roth, S. Gomes, S. Roth, Low-velocity impact loadings on mechanical components: Subtractive versus additive manufacturing, Mechanics Research Communications, Volume 90, 2018, Pages 47-51,
[19]	JC Hastie, ME Kartal, LN Carter, MM Attallah, DM Mulvihill (2020). Classifying shape of internal pores within AlSi10Mg alloy manufactured by laser powder bed fusion using 3D X-ray micro computed tomography: Influence of processing parameters and heat treatment. Materials Characterization 163, 110225
[20]	JC Hastie, J Koelblin, ME Kartal, MM Attallah, R Martinez (2021). Evolution of internal pores within AlSi10Mg manufactured by laser powder bed fusion under tension: As-built and heat treated conditions. Materials & Design 204, 109645
[21]	J Koelblin, JC Hastie, ME Kartal, A Siddiq, MM Attallah (2022). Deformation of AlSi10Mg parts manufactured by Laser Powder Bed Fusion: In-situ measurements incorporating X-ray micro computed tomography and a micro testing stage. Procedia Structural Integrity 35, 168-172

[22]	H. Hadidi, B. Mailand, T. Sundermann, E. Johnson, G. Madireddy, M. Negahban, L. Delbreilh, M. Sealy, Low velocity impact of ABS after shot peening predefined layers during additive manufacturing, Procedia Manufacturing, Volume 34, 2019, Pages 594-602
[23]	L. Hitzler, C. Janousch, J. Schanz, M. Merkel, B. Heine, F. Mack, W. Hall, A. Öchsner, Direction and location dependency of selective laser melted AlSi10Mg specimens, Journal of Materials Processing Technology, Volume 243, 2017, Pages 48-61
[24]	P. Maroti, P. Varga, H. Abraham, G.Falk, T. Zsebe, Z. Meiszterics, S.Mano, Z. Csernatony, S. Rendeki, M.Nyitrai, Printing orientation defines anisotropic mechanical properties in additive manufacturing of upper limb prosthetics, 2018, Materials Research Express, Volume 6, Number 3
[25]	P.Honarmandi, H.Xu, Study of Printing Orientation on Mechanical Properties in Additive Manufacturing Process,ASME 2019 International Mechanical Engineering Congress and Exposition, 2019
[26]	Y. Kok, X.P. Tan, P. Wang, M.L.S. Nai, N.H. Loh, E. Liu, S.B. Tor, Anisotropy and heterogeneity of microstructure and mechanical properties in metal additive manufacturing: A critical review, Materials & Design, Volume 139, 2018, Pages 565-586,
[27]	A .Abderrachid , E.L. Abdelouafi Comportement vibratoire d'une poutre encastrée sous différentes conditions d'appui à l'extrémité 24ème Congrès Français de Mécanique Brest, 2019
[28]	H. Sönnerlind COMSOL Damping in structural Dynamics : Theory and Sources, 2019 https://www.comsol.com/blogs/damping-in-structural-dynamics-theory-and-sources/
[29]	F. Li, H. Peng, X. Sun, J. Wang, G. Meng, Wave Propagation Analysis in Composite Laminates Containing a Delamination Using a Three-Dimensional Spectral Element Method, Hindawi Publishing Corporation Mathematical Problems in Engineering Volume 2012, Article ID 659849, 19 pages
[30]	A. Modir I. Tansel, Wave Propagation and Structural Health Monitoring Application on Parts Fabricated by Additive Manufacturing, Automation 2021, 2, 173–186.
[31]	B. S. Vien, W. K. Chiu, L.R. F. Rose Experimental Investigation of Second-Harmonic Lamb Wave Generation in Additively Manufactured Aluminum, ASME Nondestructive Evaluation Nov 2018Volume 1, Issue 4, 041003,
[32]	R. Velmurugan, Andrew J.J., Schneider J., Ubaid J., Gupta N.K., Sampath Kumar TS Energy absorption characteristics of additively manufactured plate-lattices under low- velocity impact loading https://dx.doi.org/10.1016/j.ijimpeng.2020.103768
[33]	A.Tridello, J.Fiocchib, C.A.Biffic, G.Chiandussid, M.Rossettoe, A.Tuissif, D.S. Paolinog, Effect of microstructure, residual stresses and building orientation on the fatigue response up to 109 cycles of an SLM AlSi10Mg alloy Elsevier International Journal o fatigue Volume 137, 2020, 105659
[34]	ASTM E1876 – 09, Standard Test Method for Dynamic Young's Modulus, Shear Modulus, and Poisson's Ratio by Impulse Excitation of Vibration, In: ASTM – Int'l, USA, (2012)
[35]	V. A. Chirikov, D. M. Dimitrov, Y.S. Boyadjiev, Determination of the Dynamic Young's Modulus and Poisson's Ratio Based on Higher

	Frequencies of Beam Transverse Vibration, Procedia Manufacturing, Volume 46, 2020, Pages 87-94,
[36]	S.Spinner, W. E Tefft,.," A Method for Determining Mechanical Resonance Frequencies and for Calculating Elastic Moduli from These Frequencies," Proceedings, ASTM, 1961, pp. 1221–1238.

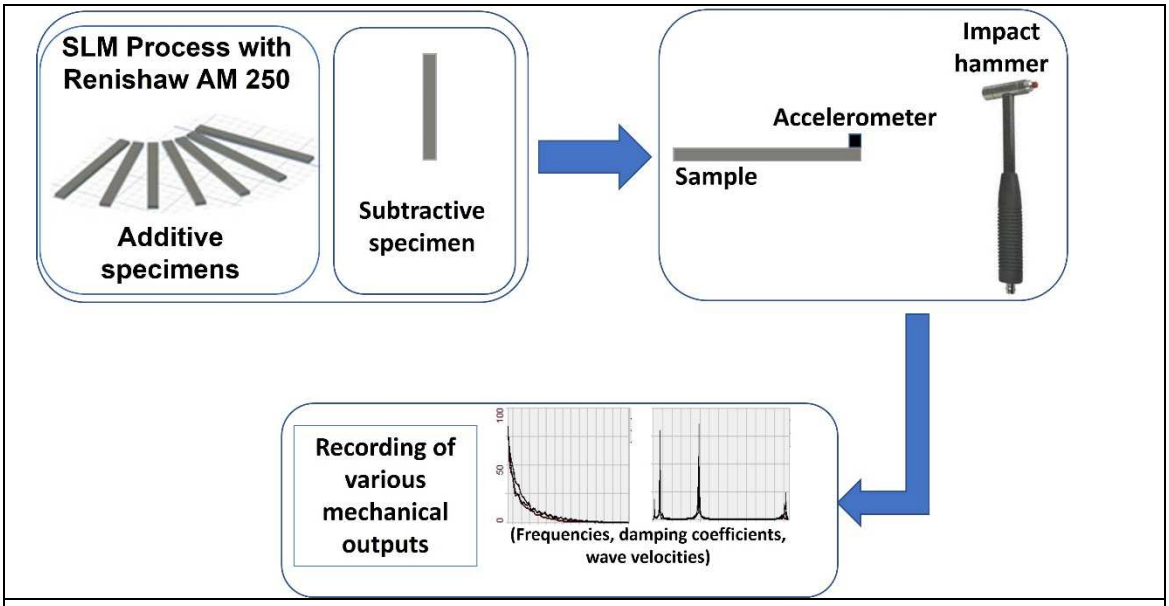

Figure 1: flowchart of the dynamical characterization process

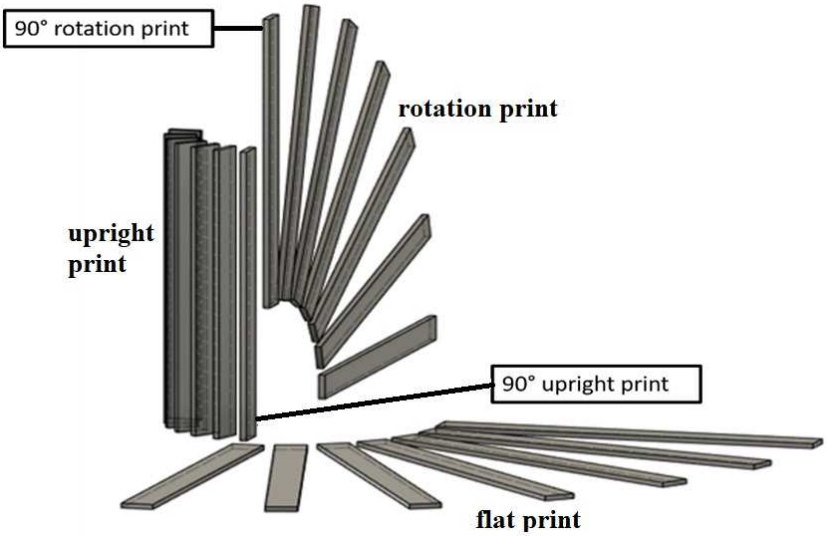

Figure 2: various orientations used for the printing of the specimen

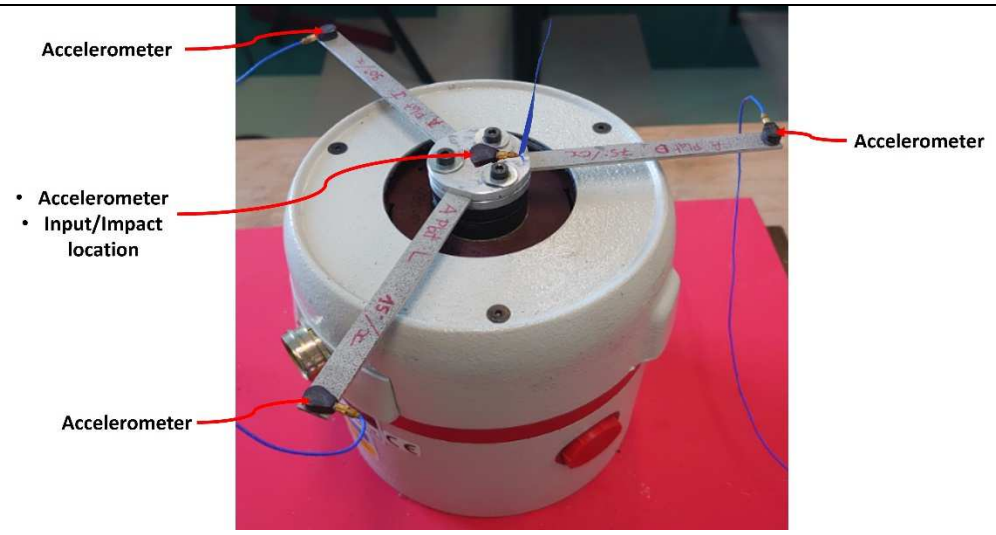

Figure 3: Dynamic mechanical experimental device

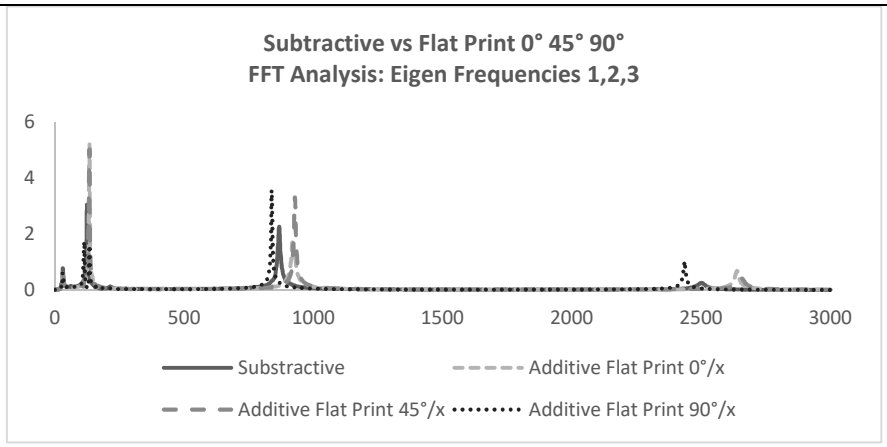

(a)

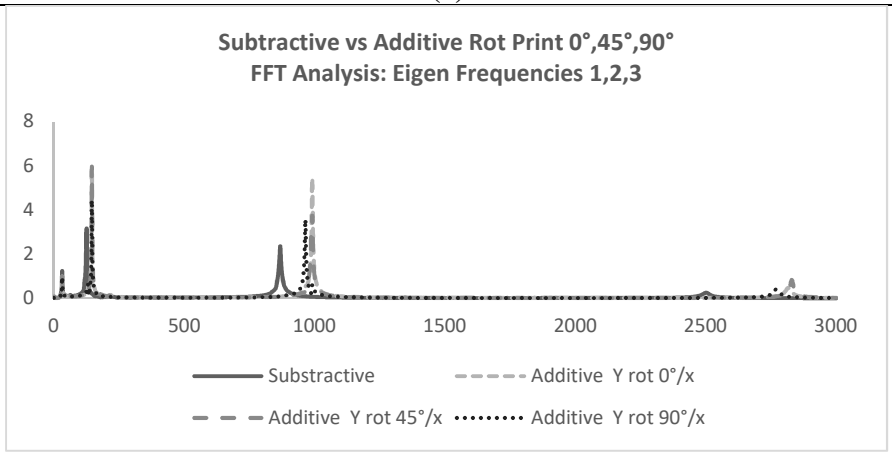

(b)

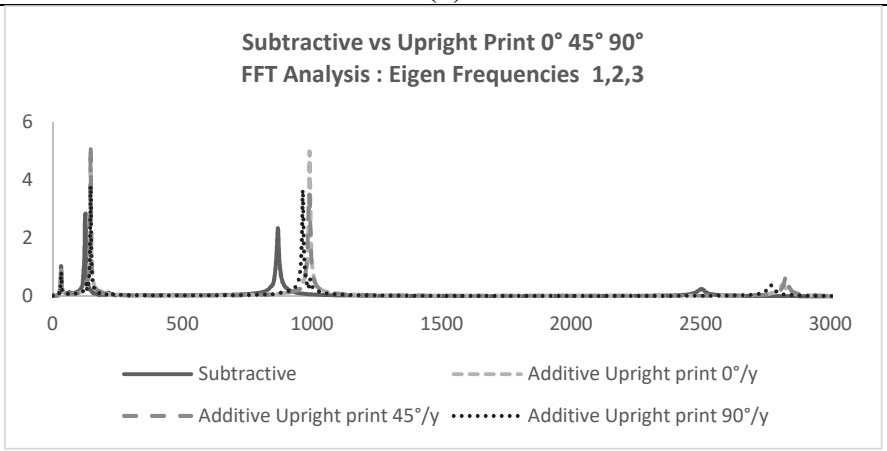

(c)

Figure 4: Frequential results of the three different printing orientations (Rotation, Upright, Flat) compared to subtractive sample.

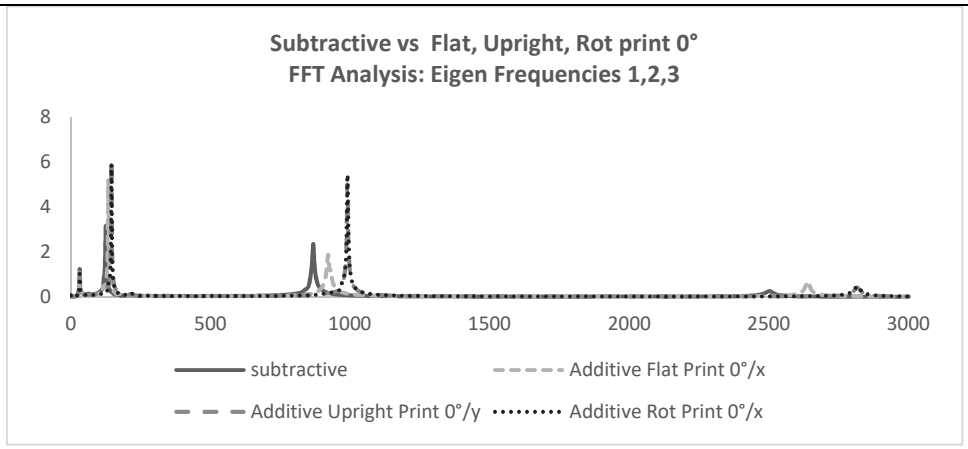

(a)

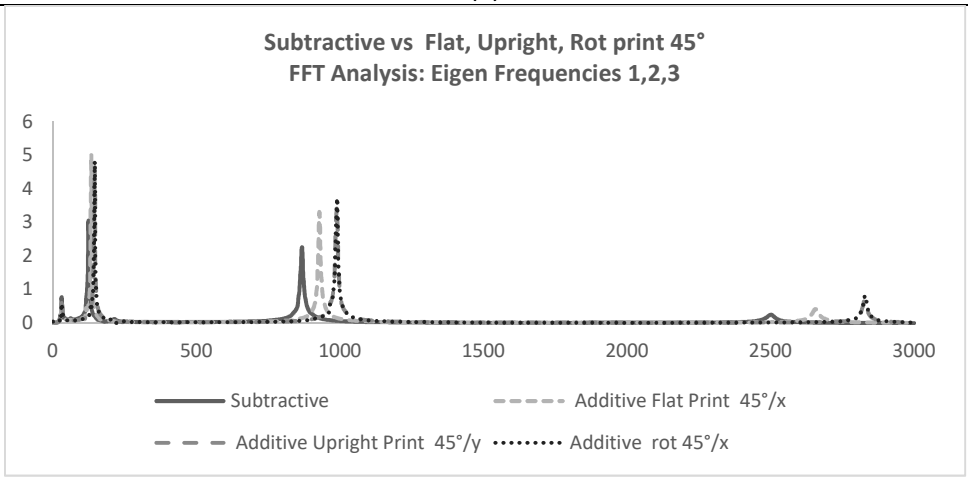

(b)

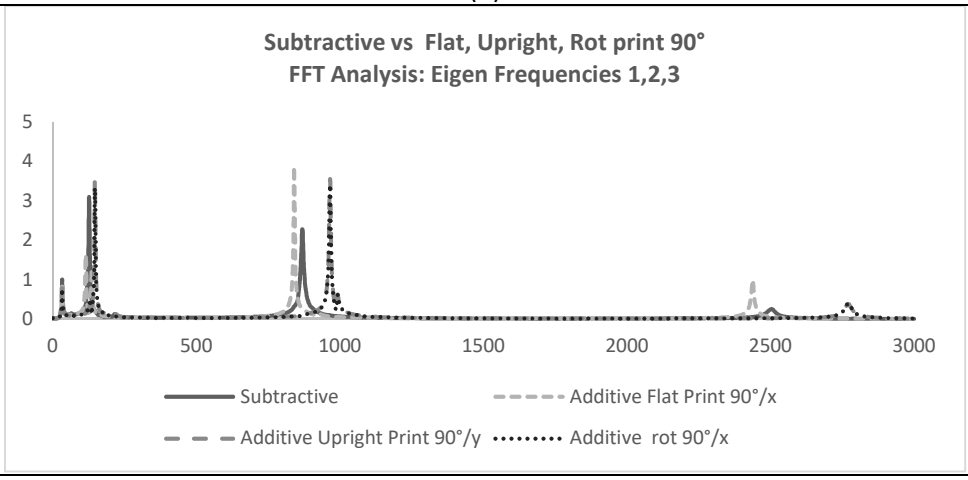

(c)

Figure 5: Frequential results of various angle for a given printing orientation

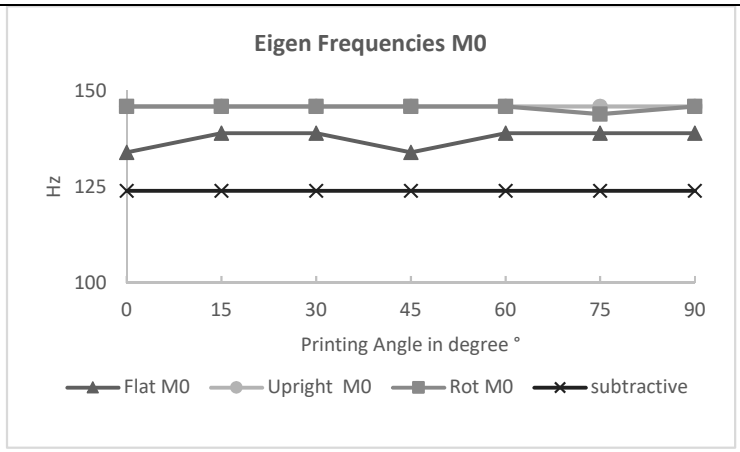

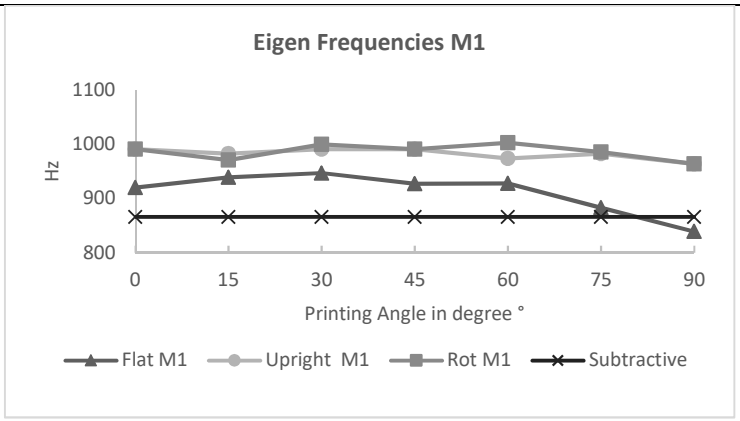

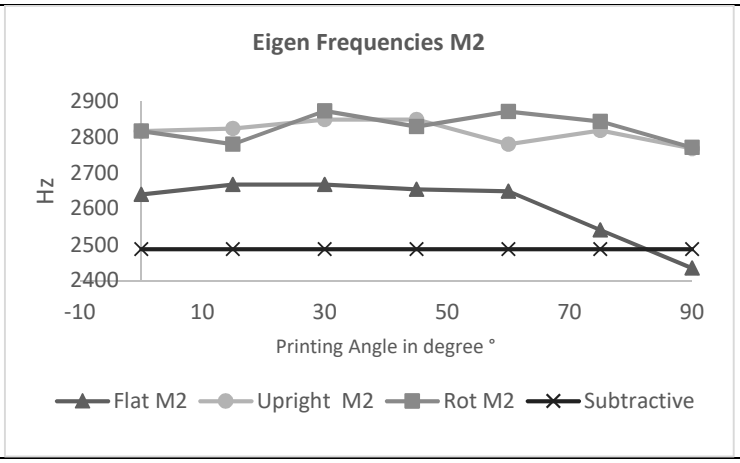

Figure 6: Frequency results M0, M1, M2, as a function of angles for different printing orientation.

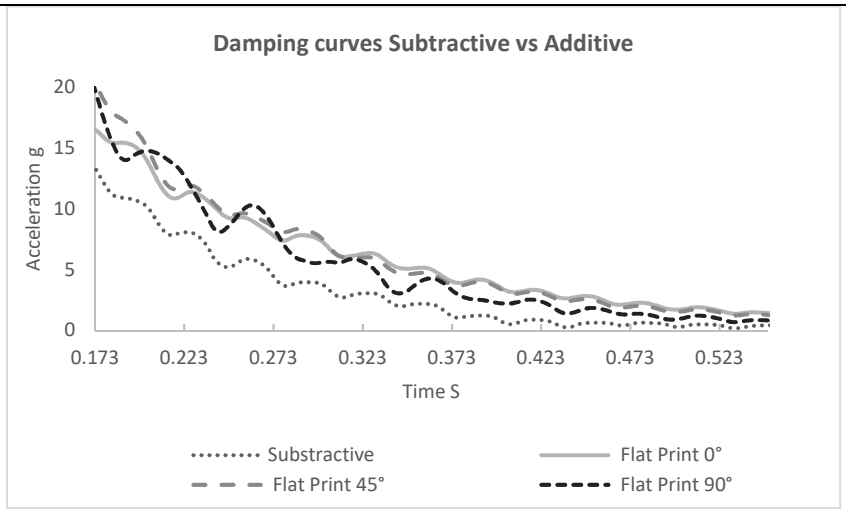

(a)

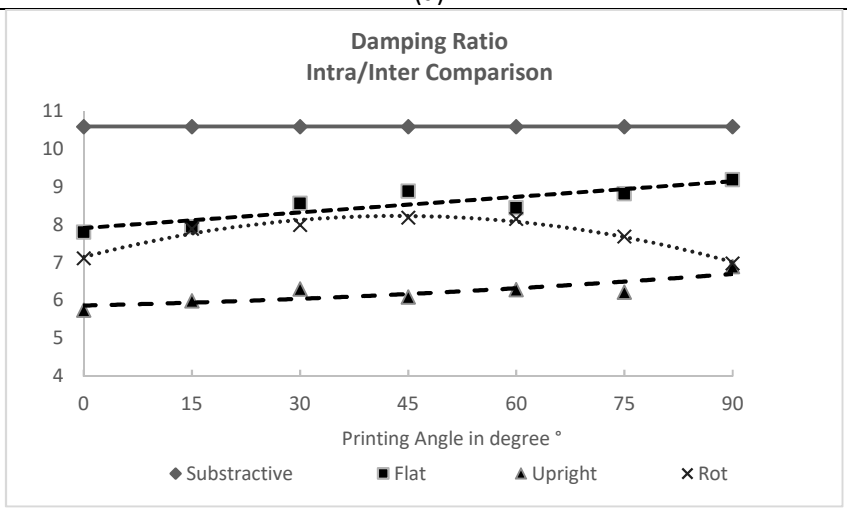

(b)

Figure 7: Damping results for various angle and various printing orientation

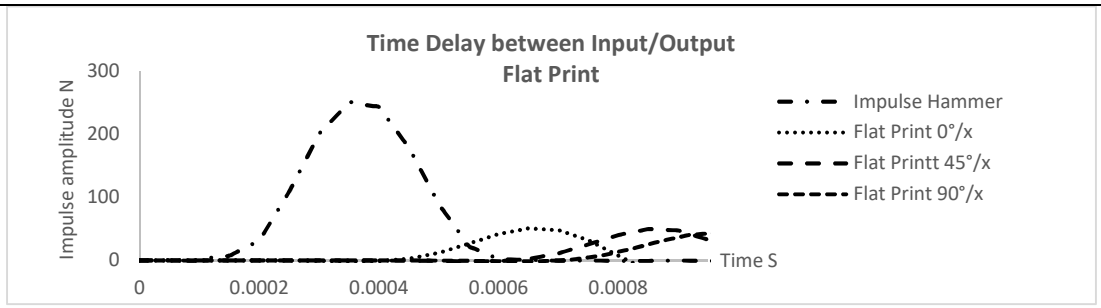

(a)

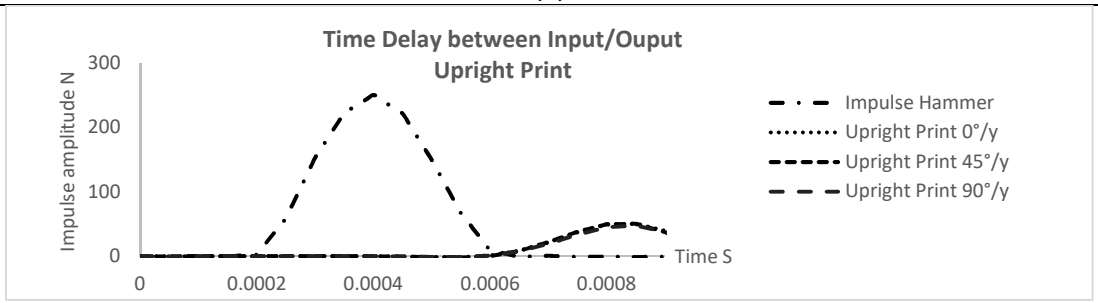

(b)

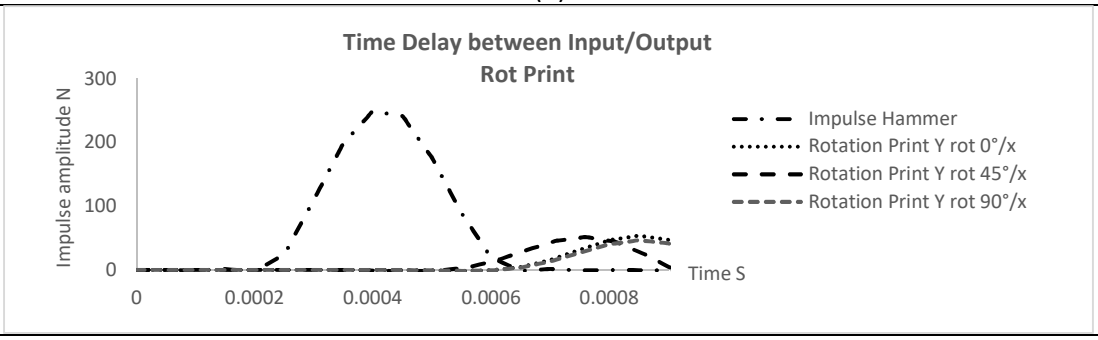

(c)

Figure 8: Time interval between input and outputs for various samples.

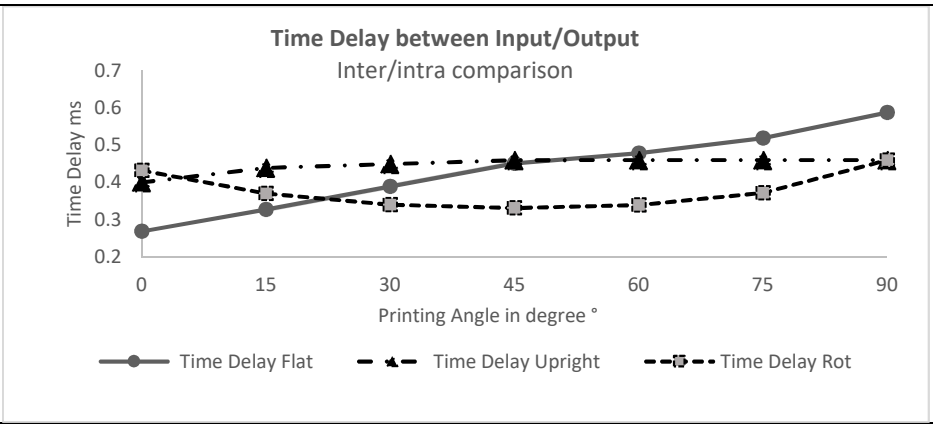

Figure 9: Time interval for the three printing orientation at various angles.

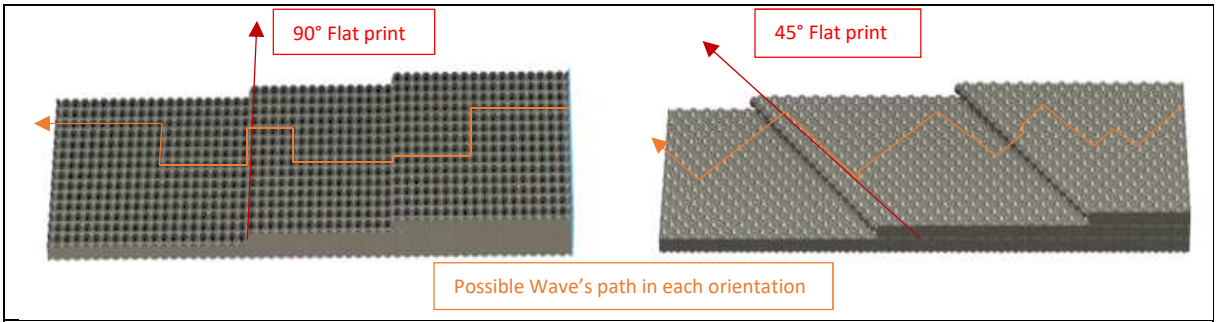

Figure 10: Wave's path comparison

Addtive Process		
Upright Printing Orientation	Flat Printing Orientation	Rotation Printing Orientation
0°, 15°, 30°, 45°, 60°, 75°, 90°		

Table 1 : printing configuration of each 3D specimen

	Flat Hz			Upright Hz			Rotation Hz			Subtractive Hz		
	M0	**M1**	**M2**	**M0**	**M1**	**M2**	**M0**	**M1**	**M2**	**M0**	**M1**	**M2**
0°	134	920	2640	146	991	2817	146	991	2817	125	869	2502
15°	139	939	2668	146	983	2824	146	971	2780	Not applicable		
30°	139	947	2668	146	991	2849	146	1000	2873			
45°	134	927	2655	146	991	2829	146	991	2829			
60°	139	928	2649	146	974	2780	146	1003	2871			
75°	139	883	2541	146	983	2819	144	986	2844			
90°	134	839	2435	146	964	2768	146	964	2771			

Table 2: General overview of natural frequencies

Orientation °	Time Delay Flat ms	Time Delay Upright ms	Time Delay Rot ms	Time Delay Subtractive ms
0	0,2688	0,40025	0,4321	0,3005
15	0,3278	0,4395	0,3707	
30	0,3892	0,4493	0,3401	
45	0,4514	0,4604	0,3315	
60	0,479	0,46042	0,34	
75	0,5193	0,46042	0,372	
90	0,5881	0,46042	0,4602	

Table 3: General overview of time delay between Input/output